

Growth of anisotropic one-dimensional ZnS nanostructures†

Daniel Moore and Zhong L. Wang*

Received 2nd June 2006, Accepted 20th June 2006

First published as an Advance Article on the web 30th June 2006

DOI: 10.1039/b607902b

Anisotropic growth in nanomaterials can lead to many interesting growth morphologies. This is especially true when the crystal structure contains anisotropy not only due to different surface plane energies but also due to surface polarity and/or chemical activity. Such is the case with wurtzite ZnS. This feature article covers the ZnS one-dimensional nanostructures that have been synthesized by a vapor–solid process, focusing on nanowires, nanorods, nanobelts, nanohelices and other derived nanostructures. This feature article mainly focuses on the polar surface dominated growth phenomena and the understanding of their formation mechanisms.

1. Introduction

Because of the ability to synthesize them in numerous configurations, II–VI semiconducting materials have attracted great interest in recent years.^{1–14} ZnS is a direct wide bandgap (3.91 eV) compound semiconductor with a high index of refraction and a high transmittance in the visible range, and it is one of the more important materials in photonics research.^{15,16} As a one-dimensional nanostructure, ZnS has been synthesized as nanowires, nanobelts, and nanocombs.^{7,10,16–26} Recently, ZnS nanobelts have been doped with manganese for possible application in spintronics.²⁶ Also, optically pumped lasing has been shown in single ZnS nanobelts.⁷ To cover the many advances in the study of ZnS, this feature article is about the one-dimensional nanostructures of ZnS and their formation mechanisms. We mainly focus on the structure analysis of the novel growth configurations. We anticipate inspiring interest in studying the novel physical, optical and chemical properties of ZnS nanostructures.

School of Materials Science and Engineering, Georgia Institute of Technology, Atlanta, GA, 30332-0245, USA.

E-mail: zhong.wang@mse.gatech.edu

† This paper is part of a *Journal of Materials Chemistry* theme issue on Anisotropic Nanomaterials. Guest editor: Luis Liz-Marzan.

2. Crystallographic structures of ZnS

In its bulk form, ZnS is typically found to have the zinc blend crystal structure at room temperature.²⁷ The zinc blend structure is cubic (Fig. 1). At elevated temperatures, bulk ZnS can undergo a phase transformation from the cubic zinc blend structure to a hexagonal crystal structure known as the wurtzite structure (Fig. 1). This transformation has been shown to occur at 1020 °C. The zinc blend and wurtzite structures are very similar. The stacking sequence of the close-packed planes of zinc blend (the (111) planes) is represented by the ABCABCABCABC repeating pattern. However, if the close-packed planes stack themselves in the ABABABABAB repeating pattern, they would form the (0001) planes of the wurtzite structure. Wurtzite has a hexagonal unit cell (space group $P63mc$). The structure of ZnS can be described as a number of alternating planes composed of tetrahedrally coordinated S^{2-} and Zn^{2+} ions, stacked alternately along the c -axis. The tetrahedral coordination in ZnS results in a non-centrosymmetric structure and piezoelectricity. A common characteristic II–VI semiconductors share is a propensity to form into the wurtzite crystal structure when their sizes are small.¹⁴ Wurtzite is the most stable structure for CdS and CdSe and the other II–VI



Daniel Moore

Daniel Moore received his BS in Physics and Mathematics from the University of Chicago in 2001. He is currently a PhD candidate in the School of Materials Science and Engineering, Georgia Institute of Technology. His research has been focused on synthesis and characterization of one-dimensional nanostructures.

Dr Zhong Lin (ZL) Wang is a Regents' Professor, COE Distinguished Professor and Director, Center for



Zhong L. Wang

Nanostructure Characterization and Fabrication, at Georgia Tech. He has authored and co-authored four scientific reference and textbooks and over 440 peer reviewed journal articles, 45 review papers and book chapters, edited and co-edited 14 volumes of books on nanotechnology, and held 12 patents and provisional patents. He is in the world's top 25 most cited authors in nanotechnology from 1992–2002. His entire publications have been cited over 12 000 times.

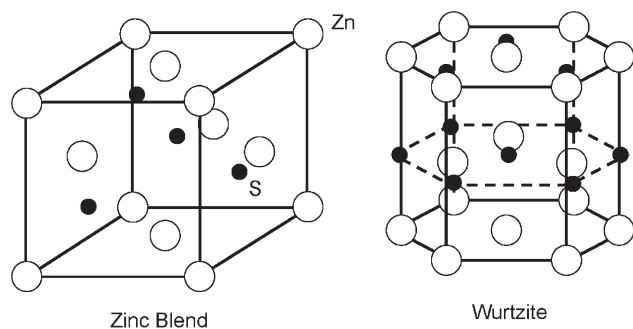


Fig. 1 The zinc blend (left) and wurtzite (right) crystal structures of ZnS.

semiconductors have previously been observed to exhibit the wurtzite crystal structure.^{22,28,29}

Another important characteristic of ZnS is the polar surfaces. The most common polar surface is the basal plane. The oppositely charged ions produce positively charged Zn-(0001) and negatively charged S-(000 $\bar{1}$) polar surfaces, resulting in a normal dipole moment and spontaneous polarization along the c -axis as well as a divergence in surface energy. Wurtzite ZnS produces anisotropic growth for two reasons. One is merely that different crystallographic planes have different surface energy. Another reason is the surface polarity and chemical activities.

Structurally, ZnS has three types of fast growth directions: $\langle 2\bar{1}\bar{1}0 \rangle$; $\langle 01\bar{1}0 \rangle$; and $\pm[0001]$. Together with the polar surfaces due to cation/anion termination, ZnS exhibits a wide range of novel structures by tuning the growth rates along these directions. The non-centrosymmetry in wurtzite gives rise to piezoelectricity,³⁰ which has been used for fabricating cantilevers for scanning probe microscopy.³¹ Nanocantilevers could be used in mass, biological, force, thermal, pressure, and chemical sensing applications.^{32–34} Through the successful synthesis of II–VI semiconductors in a nanobelt form, a wide range of mechanical and optoelectronic application may be possible for these materials. This is why II–VI semiconductors and ZnS remain a fast developing area of research.

3. Anisotropy due to polarity and differently terminated surfaces

Wurtzite ZnS has several facets that terminate with either a positively charged Zn cation or, on the opposite side, a negatively charged S anion. This characteristic of the crystal structure creates polarized surfaces, resulting in a dipole moment and spontaneous polarization along the axis perpendicular to the plane. One plane is the basal plane: (0001). Though in the bulk this dipole and divergence in surface energy is compensated for by creating facets and/or massive surface reconstruction, it can be a significant contributor to asymmetric growth in nanostructures.^{35,36} By projecting the wurtzite ZnS crystal along the $[1\bar{2}10]$ direction we can see that another set of polar surfaces are $\{01\bar{1}1\}$ (see Fig. 2).

In addition to the dipole moment contributed by the polar surfaces, the Zn- and S-terminated surfaces exhibit very different chemical activities.^{17,37,38} The Zn-terminated surface

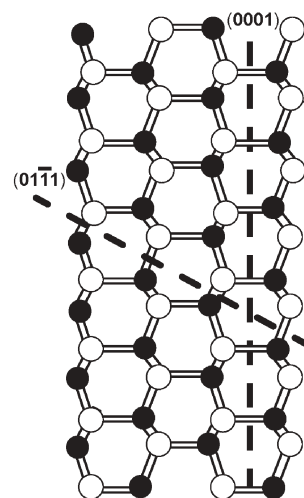


Fig. 2 Projection of the wurtzite crystal structure along $[1\bar{2}10]$. The (0001) and (01 $\bar{1}$ 1) polar planes are evident.

is chemically active and is easy to grow new nanostructures onto it, but the S-terminated surface is relatively inert.

4. Synthesis methods

Several methods have been developed to synthesize one-dimensional nanostructures of II–VI semiconductors. Among these are thermal evaporation,^{21,24,25} laser ablation,^{28,39,40} arc discharge,⁴¹ chemical synthesis methods,⁴² and self-assembly methods.⁴³ The most important group of these methods is the deposition-based synthesis methods. Members of this group include thermal evaporation methods (physical and chemical vapor deposition), laser-assisted growth, and arc discharge. The essential nature of these methods is that, from a source, a molecular “growth” species is created in a vapor form. This species is then transported to a substrate where it deposits and forms the nanostructure.

The most common deposition-based synthesis methods are physical and chemical vapor deposition (PVD and CVD).^{4,20,44} Both methods consist of the physical transport of the vapor species to the deposition site. In the case of PVD, the vapor species is typically created through the thermal evaporation of a source that is a bulk version of the desired nanomaterial. Most of these materials are commercially available in powder or chunk form. The main benefit of PVD is that it can provide for easy control over the chemistry of the synthesized material, with relatively little control of the system parameters. In the case of CVD, the vapor species is created through a chemical reaction. For example, a Zn source may be evaporated and reacted with a H_2S flow gas to form a ZnS vapor species.²⁴ However, because of the chemical reaction involved, controlling the atmosphere is extremely important with CVD and achieving the correct setup can be very difficult. This is especially true when attempting to remove residual oxygen from a system. The benefit of CVD is that it typically can be synthesized with much lower initial temperatures than with PVD.⁴⁵

Another synthesis method that allows for much lower initial temperatures is laser-assisted deposition or laser ablation. In

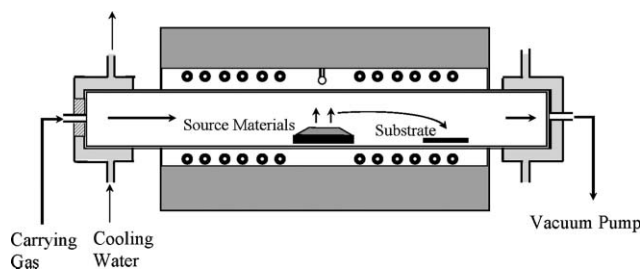


Fig. 3 Schematic of single-zone tube furnace for vapor–solid growth.

this, the source material is bombarded with a high energy laser pulse. This laser pulse provides the energy to create the vapor species as well as much of the kinetic energy needed to transport the vapor species to the deposition substrates. Because the energy causing the vaporization is provided by the laser, much lower temperatures are needed. Laser-assisted deposition also assures that the vapor species will have the same stoichiometry as the source.^{46,47}

For many of the ZnS structures synthesized, particularly those presented in this feature article, a simple vacuum tube furnace is used (Fig. 3). The source materials are placed in the center of a single-zone horizontal tube furnace, where the atmosphere, evaporation time, pressure, and temperature are controlled. The deposition substrates are placed downstream in a lower temperature region in the furnace, which is kept at a reasonable vacuum. After evacuation to a pressure of about 2×10^{-3} Torr, the temperature in the center of the tube is elevated to a controlled temperature at a specific rate depending on the source material and desired growth. An inert gas flow such as argon or nitrogen is introduced into the system to act as a carrying gas. The pressure in the system is allowed to increase and is controlled for a specific amount of time until the desired growth is achieved. When synthesis is finished, the gas flow is turned off, the vacuum is reapplied, and the furnace is allowed to cool to room temperature.

5. Kinetic controlled growth

Nanostructures are formed by altering the thermodynamic processes that normally form bulk crystals. In the early 1960s, Hill introduced extra terms into traditional thermodynamic equations to account for the formation of small structures and to enable a discussion of the processes that occur on such a small scale.⁴⁸ This is necessary because nanoscale systems have unique properties. One of the most well-known characteristics is the high surface-to-volume ratio. Because of this, the surface effects that could be neglected with bulk thermodynamics cannot be ignored in nanoscale theories. There are several different approaches to solving this issue. One way is to look at fundamental theorems of thermodynamics and introduce new functions that take into account the effects of the nanoscale system.

Another approach is to consider the system as kinetically driven. This involves looking at the various steps of growth and determining the impact that each has on the overall growth products. Often, this involves determining, among other factors, the rate-limiting steps of the growth process and

the rates at which they ensue and the impact of vapor concentration at each step.

These challenges of growth have brought some difficulty in developing a coherent model of deposition-based growth of nanostructures. However, some basic steps in deposition based growth can be outlined. First, the source diffuses from the source to the deposition substrate in the form of a vapor. Typically, this diffusion is assisted by some carrier gas or other mechanism. Second, the vapor species adsorbs and desorbs onto and from the growing surface. The vapor species can also dissociate while it is on the growth surface. Depending on the vapor species and the surface, this may even be an energetically favorable occurrence. Here, the growth surface is at first the deposition substrate but then is the surface of the growing nanostructure. Third, the adsorbed growth species undergoes surface diffusion in which it is either included into a growth site and continues the growth of the nanostructure or it escapes from the surface. Fourth, the surface grows by including the adsorbed species into the crystal structure. Finally, by-product chemicals either diffuse or desorb from the growth surface. In addition to these processes, the presence of a metallic catalyst makes it possible for the vapor species to diffuse through the liquid catalyst particle and form the nuclei.⁴⁹

Often, a metallic catalyst such as gold is used to initiate growth. The main benefit of adding a catalyst is that the growth of the nanostructures can be achieved at site-specific locations. Growth without a catalyst occurs with an initial source temperature of around 1050 °C for ZnS nanobelts. Growth of ZnS nanobelts with a catalyst has been achieved with an initial source temperature as low 850 °C.¹⁰

6. Novel anisotropic ZnS nanostructures

Anisotropic wurtzite ZnS nanostructures can be divided into two main categories: the non-polar surface dominated nanostructures and the polar surface dominated nanostructures.

6.1 Non-polar surface dominated ZnS nanostructures

Non-polar surface dominated nanostructures consist of those structures in which the polar surfaces plays relatively little role in their morphology. We can generally divide these structures into three distinct categories: nanowires, nanorods, and nanobelts (left in Fig. 4). Typically, ZnS nanowires are relatively very long, flexible, and have a circular cross-section.¹⁶ ZnS

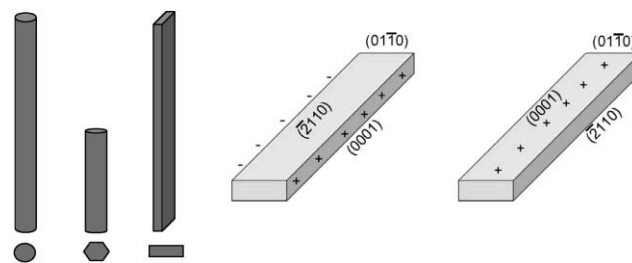


Fig. 4 (Left) Schematic examples of nanowires, nanorods, and nanobelts along with their representative cross-sections; (right) two specific cases of nanobelt crystallographic configurations that can lead to significant differences in growth.

nanorods are shorter (and therefore stiffer) and, though circular cross-sections are prevalent, can often have hexagonal cross-sections.⁵⁰ When hexagonal cross-sections are present, the surfaces of the nanorods are well-faceted. ZnS nanobelts, or “nanoribbons,” have rectangular cross-sections and are generally very flexible.^{51,52} This means that they have one main “fast” growth direction and a secondary growth direction. They have faceted surfaces (right-hand side in Fig. 4).

6.2 ZnS nanowires/nanorods

ZnS nanowires/nanorods have been synthesized by several groups.^{12,19–21,23} Meng *et al.* have grown ultrafine ZnS nanowires on gold-coated silicon substrates.²¹ Moore *et al.* have used CdSe as a buffer to grow orientation aligned bundles of ZnS nanowires.²³ The top-down view of the highly aligned nanowires can be seen in Fig. 5a. The orientation aligned ZnS nanowires bundles are formed by a two step vapor deposition process. The first step deposits the CdSe base and the second step forms the ZnS nanowires bundles, as seen in Fig. 5b. In the growth, bundles of ZnS nanowires grow on the top of a layer of CdSe, which serves as a buffer between the Si(111) substrate and the nanowires. Each bundle maintains the fairly good faceted structure of the CdSe, preserving the shape of the top of the CdSe crystal. This indicates a comparable rate of growth of the individual nanowires. The individual nanowires are single-crystal wurtzite ZnS. The orientation alignment of the ZnS nanowires is along the [0001] direction. They also share a common side surface of $(2\bar{1}\bar{1}0)$.

The two-step process forming the nanowire bundles is unique. In the first step, the CdSe grows on the Si(111) substrate. The (0001) oriented CdSe has a six-fold symmetric *a*-plane, $(10\bar{1}0)$, with an interplanar distance of 0.372 nm, which matches well to the six-fold symmetric Si(111) substrate, with an interplanar distance of 0.384 nm, resulting in a *c*-axis oriented growth of CdSe on Si(111). Due to the lattice mismatch, single crystal thin films of CdSe are not formed.

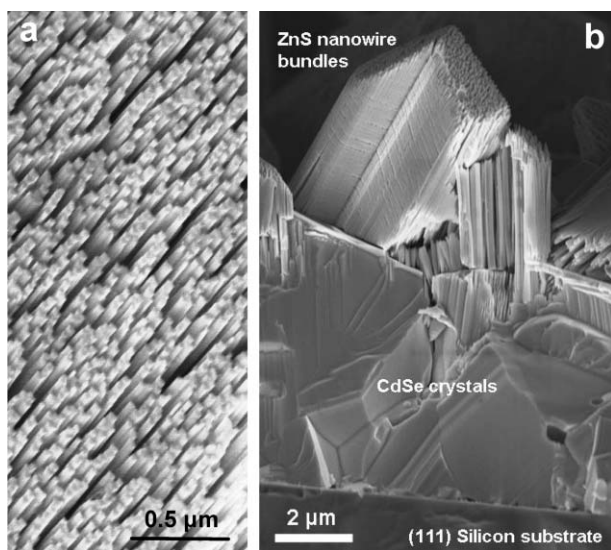


Fig. 5 (a) Top-down image of ZnS nanowire bundles. (b) Side-view SEM image of a faceted nanowire bundle, showing their growth on CdSe crystals and the (111) silicon substrate surface.

Instead, heterogeneous nucleation of CdSe results in the growth of a polycrystalline film. In the second step, the CdSe serves as a substrate for the growth of the ZnS nanowires. Because CdSe and ZnS have the wurtzite structure, ZnS growth along the *c*-axis would be preferred to minimize the lattice mismatch. All of the nanowires have the same growth rate; the morphology of the CdSe crystal is preserved. The bundles of nanowires also maintain the width and depth profile of the CdSe crystal.

ZnS nanowires and nanorods exhibit interesting properties. ZnS nanowires have been used as LEDs and shown to have long-lasting phosphorescence properties when doped with europium.^{53,54} They have also been used in forming self-organized hierarchical heterostructures and two-dimensional nanowire networks.^{55,56}

6.3 ZnS nanobelts

The successful synthesis of ZnS nanobelts was first reported in 2003 by Ma *et al.*¹⁸ Since then, several groups have reported the synthesis of ZnS nanobelts using different thermal evaporation techniques.^{24,25,57} Generally, this technique is the most common for synthesizing materials into a belt-like morphology (Fig. 6a). Using a catalyst or not in the synthesis can have an impact on the nanostructure growth as well. When synthesized without a catalyst, ZnS nanobelts tend to grow from a “weed-like” structure, as in Fig. 6b. However, the use of gold catalysts can be very effective in controlling the sites of growth, as in Fig. 6c. The synthesized nanobelts are wurtzite in structure. Though this is a meta-stable phase, the nanobelts can be left for several months without any phase

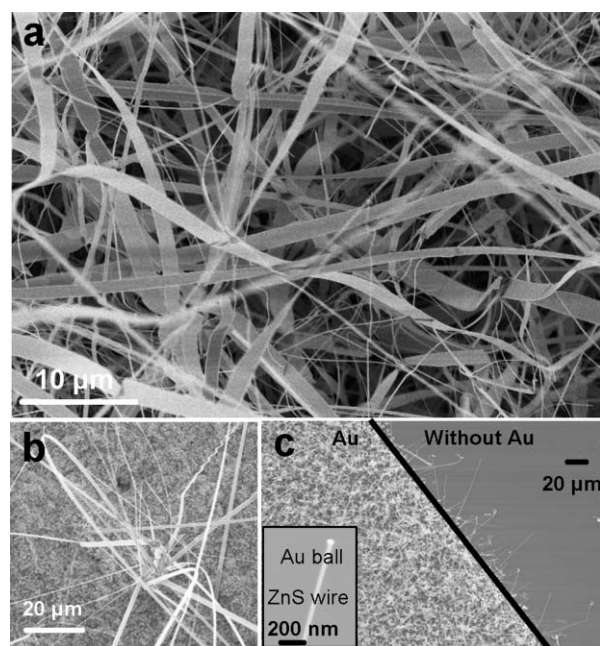


Fig. 6 (a) SEM images of ZnS nanobelts; (b) ZnS nanobelts exhibiting the weedlike growth that is typically present when no catalyst is used; (c) a deposition substrate partially covered with Au nanoparticles shows the effect of catalyst on encouraging growth on specific areas of the substrate. (inset) The Au catalyst particle is evident at the end of the ZnS nanostructure.

transformation to the zinc blend form. However, it has been shown that by bombarding a ZnS wurtzite nanobelt with an electron beam in the TEM, it is possible to locally induce the phase change from metastable wurtzite to the more stable zinc blend structure.¹⁸

Because of the faceted surface, the growth directions are very important to the properties of ZnS nanobelts. The close-packed [0001] direction is the thermodynamically fastest growth direction for the wurtzite structure. Most ZnS nanobelts are grown with the [0001] growth orientation, having (2 $\bar{1}\bar{1}0$) and (01 $\bar{1}0$) as facets as the other sides of the nanobelts. However, by changing the synthesis conditions, the growth of typically slower planes can be increased. Li and Wang, synthesized ZnS nanobelts with main growth directions of [01 $\bar{1}0$], suppressing the [0001] growth direction in certain nanobelts.²⁵ Moore *et al.* have also synthesized belts with a main growth direction along the [01 $\bar{1}0$] direction (Fig. 5).¹⁷

ZnS nanobelts have been demonstrated to have some unique properties. Zapfen *et al.* have shown that ZnS nanobelts form excellent optical cavities and have lasing modes free of a PL background even for a low pumping power density.⁷ This leads to ZnS nanobelts being useful as room temperature lasing devices. After doping with manganese using simple thermal annealing, Li *et al.* showed that the intrinsic photoluminescence peak of the ZnS nanobelts and a new peak at 585 nm gradually appear without a change in the wurtzite crystal structure.²⁶ In addition to showing a unique property of ZnS nanobelts, this provides a pathway to simple doping of nanostructures.

The mechanical properties of ZnS nanobelts have also been studied. Through a nanoindentation study, Li has shown that ZnS nanobelts decrease by 52% in elastic modulus but increase by 79% in hardness when compared with bulk ZnS.⁵¹ In a similar study, Yang *et al.* have shown that the contact stiffness in ZnS nanobelts is proportional to the indentation load and there is no size effect on elastic deformation.⁵² Also, it is possible to “cut” the nanobelts through indentation, suggesting a possible path towards manipulation of the structures.^{31,52}

6.4 Polar surface dominated ZnS nanostructures

Because of the polarity of some of the low energy surfaces of the wurtzite crystal, nanostructures that are dominated by those surfaces can show some very unique characteristics. This has been studied extensively for ZnO.⁵⁸ Similar effects show up in ZnS nanobelts.¹⁷

In essence there are two main cases where the polar surface can have a large impact on the nanostructure morphology (right-hand side in Fig. 4). The first is when the polar surface is on the smaller face of the nanobelt (the side defined by the thickness of the belt), as in the first picture. Because of the polar surface and the different chemical reactivity of Zn and S, this can result in asymmetric secondary growth off the nanobelts. The second case is when the polar surface is on the larger face of the nanobelts (the side defined by the width of the belt). Here, because of the immense electrical potential that must be compensated for, the entire morphology of the nanobelt can be altered, as will be shown in section 6.6.

6.5 Asymmetric growth on ZnS nanostructures

Asymmetric growth on wurtzite ZnS was reported as so-called nanosaws (Fig. 7a,b).^{17,18} The nanosaws are interesting in that they have a rectangular cross-section, like the nanobelts. Whether comb- or saw-like, the nanosaws have a secondary growth off one side and they show relatively no secondary growth on the other side of the structure. This asymmetric growth is directly due to the anisotropic nature of the wurtzite crystal. The secondary growth occurs on the more chemically active Zn-dominated face of the nanobelts, with virtually no secondary growth on the less active S-dominated face. In a single experimental run, the comb-like, saw-toothed belts, and the regular belt structures were found in the same growth temperature range.

The growth characteristics of these structures show some real consistency. The extruding saw-teeth on the nanosaws point along the [01 $\bar{1}0$] direction, and their large surfaces are (2 $\bar{1}\bar{1}0$) (Fig. 7c). The saw teeth are defined by facets close to (01 $\bar{1}3$) and (0 $\bar{1}13$). A common feature observed is that (0001) stacking faults are usually present between the teeth and the main nanobelt. On the comb-like structures, the fingers are pointing along the [0001] direction. We know that the Zn-terminated (0001) surface is catalytically active and can induce secondary growth, while the sulfur terminated (000 $\bar{1}$) surface is relatively inert.¹⁷ Therefore, side branches in the form of saw and comb teeth grow out of the Zn-terminated surface. Moreover, because of the relative inactivity of the sulfur terminated surface, there is no secondary growth off that surface. This is why the secondary growth appears only on one side of the nanobelts.

The wurtzite structured ZnS is metastable in the bulk and it may transform to the more stable zinc blend (sphalerite) structure under certain circumstances. After the sample was illuminated for about 10 min under 200 keV electrons, the individual nanobelts showed a large increase in density of

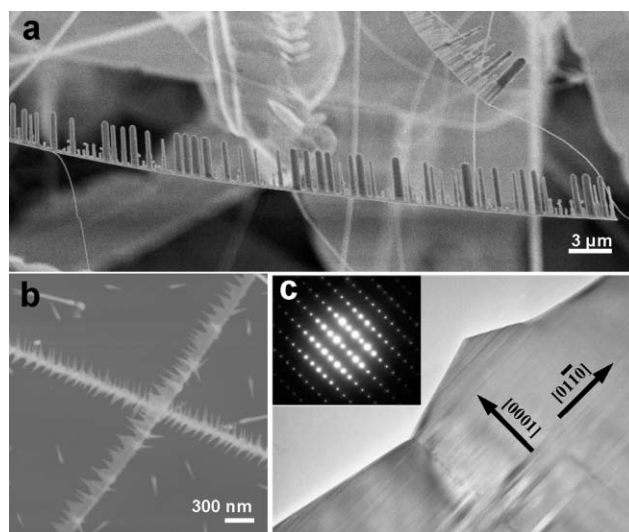


Fig. 7 (a) SEM image of a ZnS nanocomb. Notice the teeth form only on one side; (b) SEM image of a ZnS nanosaw; (c) TEM image of a ZnS nanosaw with diffraction pattern (inset) showing that the side planes are the polar (0001) surfaces, producing the sawlike structure.

planar defects. An electron diffraction pattern recorded from the area shows the co-existence of the hexagonal wurtzite structure and the cubic zinc blend structure. The orientation relationship between the two phases is: $[2\bar{1}\bar{1}0] \parallel [01\bar{1}]$, and $(0001) \parallel (111)$. The two phases co-exist by sharing the same (0001) or (111) plane. It is also known that the cubic phase ZnS typically has $\{111\}$ twins. The existence of the twins is indicated by the electron diffraction pattern, and the diffraction spots and the corresponding indexes from the hexagonal phase, the cubic phase and its twin are also illustrated by the diffraction pattern. Looking at unit cell models for the hexagonal and cubic phases of ZnS helps to illuminate their shared characteristics. The presence of the two phases in the nanobelts can be directly identified by high-resolution TEM. TEM images recorded from the hexagonal phase that is oriented along $[2\bar{1}\bar{1}0]$ match fairly well to the projected position of the Zn atoms in the unit cell.

For the close-packed configuration, there are three distinct stacking layers, named A, B and C, each of which is composed of one layer of Zn atoms and one layer of S atoms. As discussed earlier, a stacking of ABAB forms the hexagonal phase, while a stacking of ABCABC forms the cubic phase. The two structures can be transformed simply by changing the stacking sequence. The (0001) or (111) plane is the stacking plane. After illuminating a region of the ZnS nanosaw sample with the electron beam, the region is composed of two phases and a twin of the cubic phase.

Asymmetric growth on ZnS nanostructures has potential use for developing cantilevers or nanowire arrays with specific diffraction gratings—allowing for interesting optical applications.⁵⁹ Further, the different chemical potentials of the Zn-terminated and S-terminated faces provides for unique applications in photoconducting, chemical, and nanostructuring functions.^{60,61}

6.6 Helical and ring-like morphologies of ZnS nanostructures

While asymmetric growth forms so as to compensate for anisotropic polarity on the side surfaces of the nanobelts, a different mechanism exists for ZnS wurtzite nanostructures to compensate for the presence of anisotropic polarity on the main surface of the nanobelts. Helical and ring-like morphologies of wurtzite nanostructures were first reported by Kong and Wang for ZnO.³⁰ The helical structure is a particularly interesting variant of one-dimensional nanostructures as the helix is the most fundamental structural configuration for proteins, RNA, and other biomolecules. Spontaneous polarization-induced nanohelices, nanosprings, and nanorings of piezoelectric ZnO showed nanobelts that curled up during growth in order to alleviate the divergence of surface energy. Since the initial report, other related structures have been found for ZnO. These include rings and helices that form from the polar charge dominated surfaces.^{62,63} Wurtzite AlN has also been shown to form a ring structure.⁶⁴ Further, SnO₂ springs, rings, and spirals formed from polar surfaces have been reported by Yang and Wang.⁶⁵ Though SnO₂ forms the rutile structure, the helices still form as a mechanism that alleviates the excess energy present from the polar dominated surfaces.

As the cause of the formation of the helices and rings is in the crystal structure and not a chemical property of ZnO or SnO₂, wurtzite crystals have the potential to be synthesized in a helical, ring, or spiral morphology. Recently, ZnS nanohelices have been synthesized using a vapor-deposition process.⁶⁶ With ZnO and the other materials that have formed rings or helices, the structures form cleanly, without secondary or hierarchical growth off the main spine of the nanostructure. With ZnS, however, the nanohelices show significant secondary and hierarchical growth (Fig. 8a). Unlike ZnO, the ZnS nanohelices show no preferences towards handedness and no significant direct relationship between pitch and radius have been found. The most interesting aspect of the ZnS nanohelices is the hierarchical growth. The nanohelices are made of two parts. The first is the main spine which coils in a helical shape. TEM analysis shows that the main spine growth is along the $[-2110]$ direction and that the side surfaces are the $(01\bar{1}1)$ and $(0\bar{1}13)$ planes (Fig. 8b). Above, we showed that $(01\bar{1}1)$ was a polar-surface dominated plane. The second part of the nanohelix is the Y-shaped branch that grows off the main spine, towards the inside of the helix, from the $(01-11)$ plane. On this surface, secondary growth occurs out along $\sim[07-74]$. This direction is approximately perpendicular to $(01\bar{1}1)$, but because of the high energy of the direction a turn in growth to $[0002]$ leads to the formation of one of the V-branches. A twin growth by sharing the $(01\bar{1}3)$ plane (a commonly present twin in wurtzite crystals) results in the growth of the other branch (Fig. 8c).

While the formation of the helix part of the structure is well understood, the secondary growth that occurs requires further exploration. In addition to the explanation of secondary growth that is used to describe nanosaws and nanocombs, the impact of the helical shape and the polar surfaces on secondary growth must be considered. It is observed that the Y-branches are always inwards pointing to the center of the helical structure. The Zn-terminated inner surface may have a larger

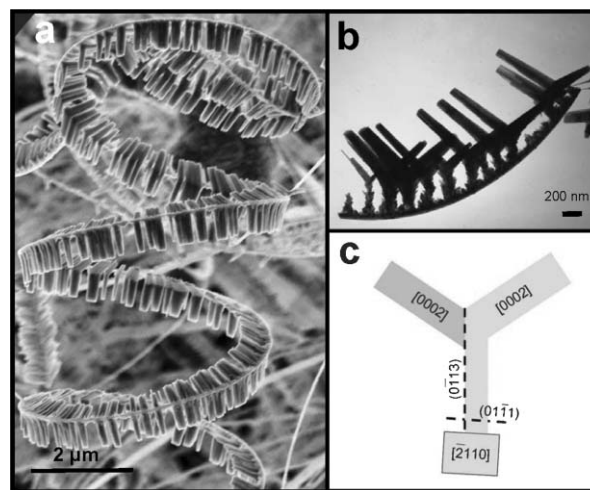


Fig. 8 (a) A typical image of a densely branched ZnS nanohelix; (b) a representative TEM image of a piece of a ZnS nanohelix that has broken off during sample preparation; (c) a model depicting the crystallographic directions present in the hierarchical structure of the ZnS nanohelix.

stress than the sulfur terminated outer surface. This may encourage secondary growth along the inside of the helix. It is also understood that the secondary growth probably all occurs after the formation of the helix, as all Y-shaped branches on an individual nanohelix grow to the same length.

7. Future avenues of research

ZnS has great potential as a useful material for nanoscale devices. This is due in particular to the anisotropic crystal structure and the wide range of structures that it can be formed in. Research investigating the properties of ZnS nanomaterials needs to be encouraged, particularly electronic and piezoelectric response properties. In particular, two directions are starting to see an increase in research and show much promise: multi-component systems and hierarchical structures.

The integration of nanotechnology with biological systems and use in medical applications is expected to produce major advances in molecular imaging, biology, and bioengineering.^{67–69} ZnS has a good recent history of use in multi-component systems, particularly in use of ZnS/CdSe quantum dot materials. The optical properties of ZnS-capped CdSe nanocrystals make them useful for optical coding of biomolecules.⁷⁰ In general, ZnS is useful for a lot of applications that require biocompatibility.⁷¹

Hierarchical nanostructures offer the potential to synthesize networks of different types of nanostructures. They also offer the opportunity to create complex structures with unique properties, such as tunable optical performance.⁷² Hierarchical structures have already been synthesized for a wide range of ZnO and other II–VI semiconductor wurtzite materials.^{72–74} The research developing the ZnS hierarchical helices is a first step in further utilizing anisotropic ZnS as a material for developing these structures.

8. Conclusion

This feature article reviews the novel nanostructures that have been formed for wurtzite ZnS. Our discussion was mainly focused on the structure and formation mechanisms of these nanostructures. Our discussion was based on three facts: crystal facets of low energies, polar surfaces formed by Zn- and S-terminated surfaces, and the distinct catalytic activities of the polar surfaces. The illustration of these fundamental growth characteristics is of importance for understanding the structure of the various growth configurations of ZnS. This will be useful for exploring novel applications of ZnS based optical and optoelectronic devices.

Acknowledgements

Research was supported by NSF, DARPA and NASA.

References

- 1 S. Q. Wang, *Appl. Phys. Lett.*, 2006, **88**, 061902–061903.
- 2 Y. P. Leung, W. C. H. Choy, I. Markov, G. K. H. Pang, H. C. Ong and T. I. Yuk, *Appl. Phys. Lett.*, 2006, **88**, 183110–183113.
- 3 S. Kumar and T. Nann, *Small*, 2006, **2**, 316–329.
- 4 S. S. Garje, J. S. Ritch, D. J. Eisler, M. Afzaal, P. O'Brien and T. Chivers, *J. Mater. Chem.*, 2006, **16**, 966–969.
- 5 C. Q. Chen, Y. Shi, Y. S. Zhang, J. Zhu and Y. J. Yan, *Phys. Rev. Lett.*, 2006, **96**, 075505–075504.
- 6 D. D. Sarma, R. Viswanatha, S. Sapra, A. Prakash and M. Garcia-Hernandez, *J. Nanosci. Nanotechnol.*, 2005, **5**, 1503–1508.
- 7 J. A. Zapien, Y. Jiang, X. M. Meng, W. Chen, F. C. K. Au, Y. Lifshitz and S. T. Lee, *Appl. Phys. Lett.*, 2004, **84**, 1189–1191.
- 8 S. Sapra and D. D. Sarma, *Phys. Rev. B*, 2004, **69**, 125304.
- 9 N. Mingo, *Appl. Phys. Lett.*, 2004, **85**, 5986–5988.
- 10 C. Ma, D. Moore, Y. Ding, J. Li and Z. L. Wang, *Int. J. Nanotechnol.*, 2004, **1**, 431–451.
- 11 V. C. Sundar, H. J. Eisler, M. G. Bawendi, T. Deng and E. L. Thomas, *Abstr. Pap. Am. Chem. Soc.*, 2003, **225**, U468–U469.
- 12 C. J. Barrelet, Y. Wu, D. C. Bell and C. Lieber, *J. Am. Chem. Soc.*, 2003, **125**, 11498–11499.
- 13 Y. W. Wang, G. W. Meng, L. D. Zhang, C. H. Liang and J. Zhang, *Chem. Mater.*, 2002, **14**, 1773–1777.
- 14 B. Ray, *II–VI Compounds*, Pergamon Press, Oxford, London, UK, 1969.
- 15 R. A. Sorel, *J. Vac. Sci. Technol., A*, 1996, **14**, 913–918.
- 16 Y. C. Zhu, Y. Bando, D. F. Xue and D. Golberg, *Adv. Mater.*, 2004, **16**, 831.
- 17 D. Moore, C. Ronning, C. Ma and Z. L. Wang, *Chem. Phys. Lett.*, 2004, **385**, 8–11.
- 18 C. Ma, D. Moore, J. Li and Z. L. Wang, *Adv. Mater.*, 2003, **15**, 228–231.
- 19 R. A. Rosenberg, G. K. Shenoy, F. Heigl, S.-T. Lee, P.-S. G. Kim, X.-T. Zhou and T. K. Sham, *Appl. Phys. Lett.*, 2005, **86**, 263115.
- 20 P. V. Radovanovic, C. J. Barrelet, S. Gradedcak, F. Qian and C. Lieber, *Nano Lett.*, 2005, **5**, 1407–1411.
- 21 X. M. Meng, J. Liu, Y. Jiang, W. W. Chen, C. S. Lee, I. Bello and S. T. Lee, *Chem. Phys. Lett.*, 2003, **382**, 434–438.
- 22 Y. W. Wang, L. D. Zhang, C. H. Liang, G. Z. Wang and X. S. Peng, *Chem. Phys. Lett.*, 2002, **357**, 314–318.
- 23 D. Moore, Y. Ding and Z. L. Wang, *J. Am. Chem. Soc.*, 2004, **126**, 14372–14373.
- 24 Y. Jiang, X. Meng, J. Liu, Z. Xie, C. S. Lee and S.-T. Lee, *Adv. Mater.*, 2003, **15**, 323.
- 25 Q. Li and C. Wang, *Appl. Phys. Lett.*, 2003, **83**, 359.
- 26 Y. Q. Li, J. A. Zapien, Y. Y. Shan, Y. K. Liu and S.-T. Lee, *Appl. Phys. Lett.*, 2006, **88**, 013115.
- 27 C. Shakin and J. Birman, *Phys. Rev.*, 1958, **109**, 818–819.
- 28 Y. Jiang, X. M. Meng, W. C. Yiu, J. Liu, J. X. Ding, C. S. Lee and S. T. Lee, *J. Phys. Chem. B*, 2004, **108**, 2784–2787.
- 29 P. Lefebvre, T. Richard, J. Allegre, H. Mathieu, A. CombetteRoos and W. Granier, *Phys. Rev. B*, 1996, **53**, 15440–15442.
- 30 X. Y. Kong and Z. L. Wang, *Nano Lett.*, 2003, **3**, 1625–1631.
- 31 W. L. Hughes and Z. L. Wang, *Appl. Phys. Lett.*, 2003, **82**, 2886–2888.
- 32 G. Y. Chen, T. Thundat, E. A. Wachter and R. J. Warmack, *J. Appl. Phys.*, 1995, **77**, 3618–3622.
- 33 J. Fritz, M. K. Baller, H. P. Lang, H. Rothuizen, P. Vettiger, E. Meyer, H. J. Guntherodt, C. Gerber and J. K. Gimzewski, *Science*, 2000, **288**, 316–318.
- 34 G. H. Wu, H. F. Ji, K. Hansen, T. Thundat, R. Datar, R. Cote, M. F. Hagan, A. K. Chakraborty and A. Majumdar, *Proc. Natl. Acad. Sci. U. S. A.*, 2001, **98**, 1560–1564.
- 35 A. R. Smith, R. M. Feenstra, D. W. Greve, J. Neugebauer and J. E. Northrup, *Phys. Rev. Lett.*, 1997, **79**, 3934–3937.
- 36 C. B. Duke, *Festkoerperprobleme—Adv. Solid State Phys.*, 1994, **33**, 1–36.
- 37 C. Ma, Y. Ding, D. Moore, X. Wang and Z. L. Wang, *J. Am. Chem. Soc.*, 2004, **126**, 708–709.
- 38 L. W. Yin, Y. Bando, J. H. Zhan, M. S. Li and D. Golberg, *Adv. Mater.*, 2005, **17**, 1972–+.
- 39 A. M. Morales and C. M. Lieber, *Science*, 1998, **279**, 208–211.
- 40 C. X. Wang, P. Liu, H. Cui and G. W. Yang, *Appl. Phys. Lett.*, 2005, **87**, 201913.
- 41 Y. J. Xiong, Y. Xie, Z. Q. Li, X. X. Li and S. M. Gao, *Chem.—Eur. J.*, 2004, **10**, 654–660.
- 42 B. Gilbert, F. Huang, Z. Lin, C. Goodell, H. Zhang and J. Banfield, *Nano Lett.*, 2006, **6**, 605–610.
- 43 B. Liu and H. C. Zeng, *J. Am. Chem. Soc.*, 2005, **127**, 18262–18268.
- 44 J. E. Mahan, *Physical Vapor Deposition on Thin Films*, Wiley-Interscience, New York, NY, 2000.

- 45 Z. X. Zhang, J. X. Wang, H. J. Yuan, Y. Gao, D. F. Liu, L. Song, Y. J. Xiang, X. W. Zhao, L. F. Liu, S. D. Luo, X. Y. Dou, S. C. Mou, W. Y. Zhou and S. S. Xie, *J. Phys. Chem. B*, 2005, **109**, 18352–18355.
- 46 P. Schenk, NIST, 2003, <http://www.ceramics.nist.gov/programs/thinfilms/PLD.html>.
- 47 H. M. Laboratories, 2006, http://huntvac.com/PLD/what_is_PLD.htm.
- 48 T. Hill, *Thermodynamics of Small Systems*, Dover Publications, NY, 2002.
- 49 G. Z. Cao, *Nanostructures and Nanomaterials: Synthesis, Properties and Applications*, Imperial College Press, London, UK, 2004.
- 50 Z.-P. Qiao, G. Xie, J. Tao, Z.-Y. Nie, Y.-Z. Lin and X.-M. Chen, *J. Solid State Chem.*, 2002, **166**, 49–52.
- 51 X. Li, X. Wang, Q. Xiong and P. C. Eklund, *Nano Lett.*, 2005, **5**, 1982–1986.
- 52 F. Yang, C. B. Jiang, W. Du, Z. Q. Zhang, S. Li and S. Mao, *Nanotechnology*, 2005, **16**, 1073–1077.
- 53 B. C. Cheng and Z. G. Wang, *Adv. Funct. Mater.*, 2005, **15**, 1883–1890.
- 54 O. Hayden, A. B. Greytak and D. C. Bell, *Adv. Mater.*, 2005, **17**, 701–707.
- 55 P. Gao, Y. Xie, L. Ye, Y. Chen and Q. Guo, *Cryst. Growth Des.*, 2006, **6**, 583–587.
- 56 G. Z. Shen, Y. Bando, C. C. Tang and D. Golberg, *J. Phys. Chem. B*, 2006, **110**, 7199–7202.
- 57 C. Borchers, D. Stichtenoth, S. Muller, D. Schwen and C. Ronning, *Nanotechnology*, 2006, **17**, 1067–1071.
- 58 Z. L. Wang, X. Y. Kong, Y. Ding, P. Gao, W. Hughes and R. Yang, *Adv. Funct. Mater.*, 2004, **14**, 943–956.
- 59 Z. W. Pan, S. M. Mahurin, S. Dai and D. H. Lowndes, *Nano Lett.*, 2005, **5**, 723–727.
- 60 T. Gao, Q. H. Li and T. H. Wang, *Appl. Phys. Lett.*, 2005, **86**, 173105.
- 61 P. A. Hu, Y. Q. Liu, L. C. Cao and D. B. Zhu, *J. Phys. Chem. B*, 2004, **108**, 936–938.
- 62 X. Y. Kong, Y. Ding, R. Yang and Z. L. Wang, *Science*, 2004, **303**, 1348–1351.
- 63 P. Gao, Y. Ding, W. Mai, W. Hughes, C. Lao and Z. L. Wang, *Science*, 2005, **309**, 1700–1704.
- 64 J. Duan, S. Yang, H. Liu, J. Gong, H. Huang, X. Zhao, J. Tang, R. Zhang and Y. Du, *J. Cryst. Growth*, 2005, **283**, 291–296.
- 65 R. Yang and Z. L. Wang, *J. Am. Chem. Soc.*, 2006, **128**, 1466–1467.
- 66 D. Moore, Y. Ding and Z. L. Wang, *Angew. Chem.*, 2006, in press.
- 67 W. C. Chan and S. Nie, *Science*, 1998, **281**, 2016–2018.
- 68 D. A. LaVan, D. M. Lynn and R. Langer, *Nat. Rev. Drug Discovery*, 2002, **1**, 77–84.
- 69 C. M. Niemeyer, *Angew. Chem., Int. Ed.*, 2003, **42**, 5796–5800.
- 70 M. Y. Han, X. Gao, J. Z. Su and S. Nie, *Nat. Biotechnol.*, 2001, **19**, 631–635.
- 71 Y. Zhang and N. Huang, *J. Biomed. Mater. Res. B*, 2006, **76**, 161–168.
- 72 J. Y. Lao, J. Y. Huang, D. Wang and Z. F. Ren, *J. Mater. Chem.*, 2004, **14**, 770–773.
- 73 X. Wang, P. Gao, J. Li, C. Summers and Z. Wang, *Adv. Mater.*, 2002, **14**, 1732.
- 74 P. X. Gao and Z. L. Wang, *J. Phys. Chem. B*, 2004, **108**, 7534–7537.